



## LETTER

# Akt3 promotes cancer stemness in triple-negative breast cancer through YB1-Snail/Slug signaling axis

Dear Editor,

Triple-negative breast cancer (TNBC) is an aggressive breast cancer subtype enriched in cancer stem cells (CSCs), which is characterized by high malignancy and drug resistance.<sup>1</sup> The PI3K/Akt signaling cascade is frequently hyperactivated in cancers. Distinct and non-redundant functions of the three Akt isoforms in tumorigenesis, however, have not been studied extensively. It is noteworthy that despite a few isoform-specific substrates have been identified for Akt1 and Akt2, an Akt3-specific substrate is yet to be discovered. We have previously shown that overexpression of Akt3, but not Akt1 or Akt2, plays an essential role in TNBC growth and therapeutic resistance of breast cancer.<sup>2</sup> However, the role of Akt3 in TNBC CSCs remains unclear.

To examine the effect of Akt3 on CSC properties, we utilized a dox-inducible Crispr/Cas9 system to knockout Akt3. Immunoblotting confirmed that Akt3, but not Akt1 or Akt2, was knockout specifically in TNBC cells (Fig. S1A). 3D spheroid growth was significantly reduced in Akt3-depleted spheroids (Fig. S1B), agreeing with our previous observation on the critical function of Akt3 in TNBC growth.<sup>2</sup> Single cell clones were then generated to assess the effect of complete Akt3 depletion on CSCs. Akt3-depleted mammospheres displayed decreased formation capacity over multiple passages (Fig. 1A; Fig. S2A). We also validated the effect of Akt3 knockout using a distinct gRNA (Fig. S2B). Akt3 depletion was found to decrease the ALDH<sup>high</sup> population by 88% and 96% in MCF10-DCIS and MDA-MB-231 cells, respectively (Fig. 1B; Fig. S2C). The percentage of CD44<sup>high</sup>/CD24<sup>low</sup> cells was also markedly reduced in Akt3-depleted cells (Fig. 1C; Fig. S2D). Among the eighteen CSC-related genes that we tested, we consistently observed downregulation of Slug and Snail mRNA in Akt3-depleted MCF10-DCIS and MDA-MB-231 cells, respectively (Fig. S2E).

Snail and Slug are homologs belonging to the SNAIL family of zinc finger transcriptional regulators. In addition to sharing a high homology in protein structure, Snail and Slug are implicated in common cellular functions, such as regulation of lineage commitment and stemness of both normal and carcinogenic cells. Indeed, protein levels of Slug and Snail were markedly downregulated in Akt3-knockout cells (Fig. 1D). This also agrees with clinical data where Akt3 expression is positively correlated with expression of Slug and Snail in breast tumor samples (Fig. S2F). The degree to which Akt3 regulates tumor-initiating ability was then assessed by limiting dilution assays. Tumor-initiating cell frequency was significantly lower in mice injected with Akt3-knockout cells (Fig. 1E). In addition, size of Akt3-depleted tumors is much smaller than those in no dox group (Fig. 1F). Akt3-knockout cells also showed attenuated tumor-initiating cell frequency in *in vitro* limiting dilution assays (Fig. S2G). These data point to an important function of Akt3 in promoting CSC formation and self-renewal.

Y box binding protein 1 (YB1, YBX1) has been demonstrated to play an important role in promoting CSC phenotypes in a variety of tumor types including breast cancer. In addition, it has been shown to be phosphorylated at Ser<sup>102</sup> by Akt,<sup>3,4</sup> but the isoform-specificity issue has not been addressed. We first analyzed the expression of YB1 and found that whereas YB1 mRNA is upregulated in TNBC tumors, its expression is underrepresented in other subtypes (Fig. S3A; TCGA Cell 2015). High expression of YB1 in TNBC cells is also validated in a panel of breast tumor lines (Fig. 1G). Furthermore, breast cancer patients with higher YB1 or Akt3 expression have significantly shorter relapse-free survival (Fig. S3B). We then explored the association of YB1 phosphorylation and Akt isoform expression using clinical datasets. Interestingly, expression of Akt3, but not Akt1 or Akt2, correlates positively with YB1 phosphorylation at Ser<sup>102</sup> (Fig. 1H). On the other hand, none of the Akt isoform positively associates with YB1 protein expression.

Peer review under responsibility of Chongqing Medical University.

<https://doi.org/10.1016/j.gendis.2022.08.006>

2352-3042/© 2022 The Authors. Publishing services by Elsevier B.V. on behalf of KeAi Communications Co., Ltd. This is an open access article under the CC BY-NC-ND license (<http://creativecommons.org/licenses/by-nc-nd/4.0/>).

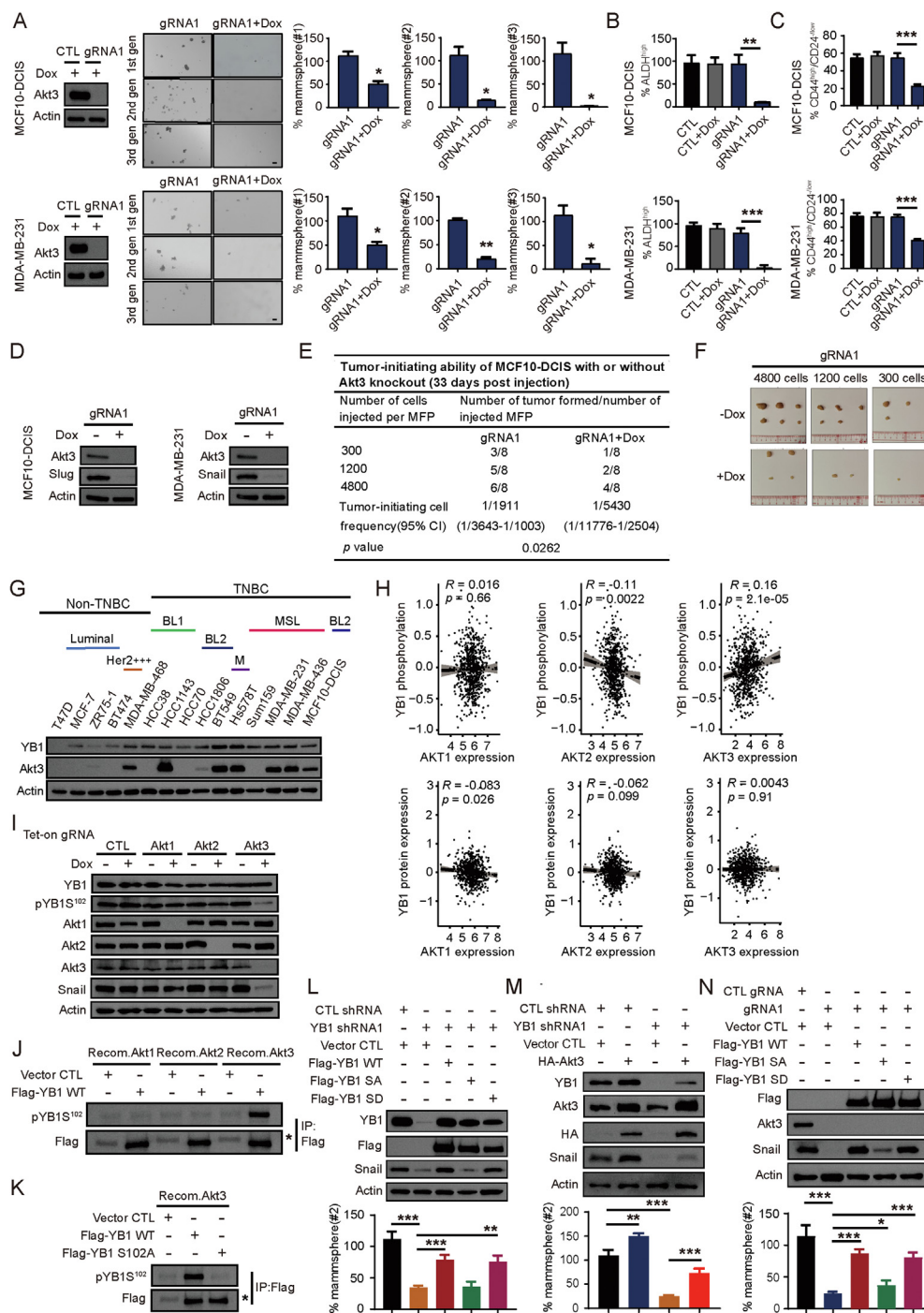


**Figure 1** Akt3 promotes TNBC stemness via YB1 phosphorylation. **(A)** MCF10-DCIS and MDA-MB-231 cells expressing tet-on Akt3 or CTL gRNA were treated with doxycycline (dox; 100 ng/mL). Left: immunoblotting was performed on lysates of single clones to confirm Akt3 knockout. Middle: Cells were seeded for first-, second-, and third-generation mammosphere-formation assay. Representative images of mammospheres are shown. Scale bar, 100  $\mu$ m. Right: Bar graphs depict the mammosphere number. **(B)** ALDH activity of MCF10-DCIS and MDA-MB-231 cells with or without Akt3 knockout, measured by AldeRed ALDH detection assay. Population of cells with high ALDH activity was quantified and depicted in bar graphs. **(C)** MCF10-DCIS and MDA-MB-231 cells with or without Akt3 knockout were labeled with anti-CD44-PE and anti-CD24-Alex 647 antibodies. Population of CD44<sup>high</sup>/CD24<sup>low</sup> cells were detected by flow cytometry. **(D)** Immunoblots showing expression levels of Slug and Snail in MCF10-DCIS and MDA-MB-231 cells with and without Akt3 knockout. Experiments were repeated twice independently with similar results. **(E)** Limiting dilution analysis of tumor-initiating cell frequency of MCF10-DCIS cells with or without Ak3 knockout. Tumor incidence was shown as number of tumor formed/number of injected MFP. Tumor-initiating cell frequency was calculated using the ELDA software. CI, confidence interval. **(F)** Pictures of MCF10-DCIS tumors. Tumors were harvested at the end of *in vivo* limiting dilution assay. **(G)** Immunoblotting showing expression of YB1 and Akt3 in a panel of breast cancer cell lines, Her2 +++, Her2-overexpressed, BL1, basal-like 1, BL2,

These observations prompted us to investigate whether YB1 is a substrate of Akt3, and their roles in TNBC CSC phenotypes.

Earlier studies have shown that Akt phosphorylates YB1 at Ser<sup>102</sup>.<sup>3,4</sup> However, myr-Akt1 was utilized, where the constitutively active Akt could be localized at a site different from endogenously expressed proteins, preclude the identification of isoform specificity. To determine whether YB1 is an Akt isoform-specific substrate, we knockout individual Akt isoform in TNBC cells (Fig. 1I; Fig. S4A). Surprisingly, only depleting Akt3 results in a robust reduction of YB1 phosphorylation as well as Slug and Snail expression (Fig. 1I; Fig. S4A). To investigate if YB1 is a direct substrate of Akt3, purified flag-tagged wild-type (WT) YB1 was incubated with recombinant active Akt isoforms in an *in vitro* kinase assay. Akt3, but not Akt1 or Akt2, efficiently phosphorylates YB1 (Fig. 1J; Fig. S4B), suggesting that there is a molecular determinant on Akt3 or YB1 which allows isoform-specific phosphorylation. We also demonstrated that Akt3 phosphorylates YB1 at Ser102, since a Ser102Ala (S102A) mutant cannot be phosphorylated by recombinant Akt3 (Fig. 1K; Fig. S4C). In addition, Akt3 depletion markedly reduces growth factor-induced YB1 phosphorylation (Fig. S4D). Collectively, these findings demonstrate that YB1 is a direct and specific substrate of Akt3.

We next investigated the contribution of YB1 to stemness potential in TNBC cells. Silencing YB1 results in reduced mammosphere formation, accompanied by decreased Slug/Snail expression (Fig. S5A). Conversely, WT Flag-YB1 overexpression results in increased mammosphere formation and Snail/Slug levels (Fig. S5B). These data are in line with previous findings, in which YB1 expression is correlated with Snail and Slug levels in breast tumors (Fig. S5C). Overexpression of S102A Flag-YB1 has no effect on mammosphere numbers, whereas phospho-mimetic Ser102Asp (S102D) mutant promotes mammosphere formation (Fig. S5B), highlighting the role of YB1 phosphorylation in CSC properties. Notably, enhanced expression of Slug/Snail was observed in cells overexpressing S102D but not S102A mutants. Using JASPAR database, we found potential YB1 binding sites on both Snail and Slug promoters. It would be interesting to test whether phosphorylated YB1 transcriptionally activates Snail/Slug by directly binding to

their promoters in future studies. We then performed rescued experiments to further determine if YB1 phosphorylation plays a critical role in mediating stemness. Whereas WT and S102D Flag-YB1 effectively rescues the mammosphere formation ability in YB1-knockdown cells, S102A YB1 has minimal effect (Fig. 1L; Fig. S6). The effects of WT and mutants of YB1 on mammospheres are corroborated with Slug and Snail expression.

As inhibition of CSC properties upon YB1 silencing phenocopies Akt3 downregulation, we next determined if promotion of stemness by Akt3 is mediated through YB1 phosphorylation. Overexpression of HA-Akt3 enhances mammosphere formation and Slug/Snail expression (Fig. 1M; Fig. S7A). Alternatively, YB1 silencing reduces mammosphere numbers. Depletion of YB1 in Akt3-overexpressed cells results in attenuated mammosphere formation as well as Slug/Snail protein levels (Fig. 1M; Fig. S7A), supporting a role of YB1 in mediating Akt3's effect on CSCs. To examine the functional significance of YB1 phosphorylation, we performed rescue studies. Whereas WT and S102D mutant of YB1 effectively reverse the mammosphere formation in Akt3-depleted cells, S102A YB1 mutant does not rescue (Fig. 1N; Fig. S7B). These data demonstrate that phosphorylation of YB1 is required for Akt3-mediated promotion of stemness.

In summary, we uncovered a novel function of Akt3 in regulating TNBC stemness via YB1-Snail/Slug signaling axis. To the best of our knowledge, we have identified YB1 as the first bona fide Akt3-specific substrate. In addition, we provided direct evidence that YB1 phosphorylation promotes Snail/Slug expression and CSC phenotypes. Our new findings provide the basis for therapeutic development in eradicating CSCs by targeting the Akt3-YB1 axis.

## Materials and methods

### Cell culture

T47D, BT474, MCF-7, MDA-MB-436, MDA-MB-468, MDA-MB-231, Hs578T, ZR-75-1, HCC38, HCC1143, HCC70, HCC1806, BT-549 and HEK293T cells were obtained from ATCC. T47D, MCF-7, MDA-MB-468, MDA-MB-231 and HEK293T cells were

basal-like 2, M, mesenchymal, MSL, mesenchymal stem-like. Experiments in G were repeated twice independently with similar results. (H) Scatterplots showing the correlation of Akt isoform expression and pYB1 Ser<sup>102</sup> levels in breast cancer samples ( $n = 719$ , TCGA-BRCA, include all breast cancer subtypes). Pearson correlation coefficients and  $p$  value are shown in each plot. (I) Immunoblotting showing expression levels of the indicated proteins in MDA-MB-231 cells with or without Akt1/2/3 knockout. (J) MDA-MB-231 cells were transfected with control vector or 3xFlag-YB1 WT in serum-free media for 24 h. Anti-Flag immunoprecipitates were used in *in vitro* assays with recombinant active Akt1/2/3 (Recom. Akt1/2/3). The kinase reaction was terminated, and samples were immunoblotted. \*IgG heavy chain. (K) MDA-MB-231 cells were transfected with control vector, 3xFlag-YB1 WT or 3xFlag-YB1 Ser102Ala (SA) in serum-free media for 24 h. Anti-Flag immunoprecipitates were used in *in vitro* assays with recombinant active Akt3. Samples of kinase reaction were immunoblotted. \*IgG heavy chain. (L) YB1-depleted MDA-MB-231 cells were infected with control vector, 3xFlag-YB1 WT, 3xFlag-YB1 Ser102Ala (SA), or 3xFlag-YB1 Ser102Asp (SD). After selection with puromycin for 10–15 days, cells were seeded for mammosphere-formation assay. Bar graphs depict the mammosphere number in 2nd generation. (M) YB1-knockdown MDA-MB-231 cells were infected with control vector or HA-Akt3 for 24 h and then subjected to mammosphere-formation assay. Whole-cell lysates were subjected to immunoblotting. Bar graphs depict the mammosphere number in 2nd generation. (N) Akt3 -knockout MDA-MB-231 cells were infected with control vector, 3xFlag-YB1 WT, SA, or SD for 24 h and then subjected to mammosphere-formation assay. Whole-cell lysates were subjected to immunoblotting. Bar graphs depict the mammosphere number in 2nd generation.  $p$  values were calculated by two-sided Student's  $t$  test in A–C, L–N. Error bars, mean  $\pm$  SD of 3 independent experiments. \* $P < 0.05$ , \*\* $P < 0.01$ , \*\*\* $P < 0.001$ .

maintained in Dulbecco's Modified Eagle medium (DMEM; Gibco) supplemented with 10% Tet system-approved Fetal Bovine Serum (FBS; Clontech). ZR-75-1, HCC38, HCC1143, HCC70, HCC1806, BT-549 cells were cultured in RPMI 1640 medium (Gibco) supplemented with 10% FBS. BT474 was maintained in RPMI 1640 medium supplemented with 10% FBS and 10  $\mu\text{g}/\text{mL}$  Insulin. Hs578T and MDA-MB-436 were maintained in DMEM supplemented with 10% FBS and 10  $\mu\text{g}/\text{mL}$  Insulin. SUM159-PT was maintained in Ham's F12 Medium (Lonza) supplemented with 5% FBS, 5  $\mu\text{g}/\text{mL}$  Insulin and 500 ng/mL Hydrocortisone. MCF10-DCIS was maintained in DMEM/F-12 (Gibco) supplemented with 5% horse serum, 20 ng/mL EGF, 10  $\mu\text{g}/\text{mL}$  Insulin, 100 ng/mL final cholera toxin and 500 ng/mL hydrocortisone. All cell lines obtained from the cell banks listed above are tested for authentication using short tandem repeat profiling and passaged for fewer than 6 months, and routinely assayed for mycoplasma contamination.

### Antibodies and growth factors

Anti-Akt1 (#C73H10), anti-Akt2 (#D6G4), anti-Akt3(#L47B1), anti-HA tag (#C29F4), anti-YB1 (#D2A11), anti-phospho-YB1(S102) (#C34A2), anti-Snail (#C15D3), anti-Slug (#C19G7) and anti-actin (#3700) antibodies were obtained from Cell Signaling Technology. Anti-FLAG (F3165) antibody was purchased from Sigma—Aldrich. Alexa Fluor® 647 Mouse Anti-Human CD24 and PE Mouse Anti-Human CD44 antibodies were purchased from BD Biosciences. Horseradish peroxidase-conjugated anti-mouse and anti-rabbit immunoglobulin G (IgG) antibodies (AP307P, AP308P) were purchased from Millipore. Cells were stimulated with Recombinant human IGF-1 and EGF (R&D Systems) were used at a final concentration of 100 ng/mL and 20 ng/mL, respectively.

### Plasmids

To knockout Akt1, Akt2, Akt3, Crispr/Cas9 knockout system was used. lentiV\_Cas9\_puro (#108100) and FgH1tUTG (#70183) were ordered from Addgene. Guide RNAs (gRNAs) was designed using online tool [www.crisprscan.org/](http://www.crisprscan.org/) and <http://crispr.mit.edu/>. gRNA oligos with sticky ends were synthesized by IDT company. Then gRNAs were cloned into BsmBI restriction site of FgH1tUTG vector. To overexpress exogenous Flag-YB1, CDS of YB1 with 3XFlag tag at N-terminal was synthesized and cloned into CD532A-1 vector by GENEWIZ. To overexpress exogenous Flag-YB(S102A), Flag-YB(S102D), CDS of YB1(S102A) or CDS of YB1(S102D) with 3XFlag tag at N-terminal was synthesized and cloned into CD532A-1 vector by GENEWIZ. Construction of HA-AKT3/pTRIPZ has been described previously.<sup>2</sup> shRNAs were cloned into pLKO.1 vector (Addgene 8453) digested by AgeI and EcoRI.

### Lentivirus infection and single cell cloning of Akt3-knockout cells

To produce lentiviral supernatants, 10  $\mu\text{g}$  lentiviral vectors (FgH1tUTG, lentiV\_Cas9\_puro, CD532A-1) were co-transfected with 7  $\mu\text{g}$  psPAX2 and 2.4  $\mu\text{g}$  VSV-G vectors to HEK293T cells, using polyethylenimine as transfection

reagent. 65 h post transfection, lentiviruses were filtered by 0.45  $\mu\text{m}$  syringe filter (Thermo fisher 7232545). 0.3–0.75 mL lentivirus with 5  $\mu\text{g}/\text{mL}$  polybrene were added to breast tumor cells for 12–24 h in a well of 6-well plates. Cells were sorted by Fluorescence-activated cell sorting (FACS) with a cell sorter (Sony) or selected with puromycin for 7–14 days. Single cell cloning was performed with limited dilution in 96-well plates. Akt3 knockout was verified by immunoblotting.

### Immunoblotting

Cells were washed with PBS at 4 °C and lysed in EBC buffer (0.5% NP-40, 120 mM NaCl, 50 mM Tris—HCl (pH 7.4), protease inhibitor cocktail, 50 nM calyculin, 1 mM sodium pyrophosphate, 20 mM sodium fluoride, 2 mM EDTA, 2 mM EGTA) for 25 min on ice. Cell extracts were pre-cleared by centrifugation at 13,000  $\times g$  for 10 min at 4 °C and protein concentration was measured with the Bio-Rad protein assay reagent using a BioTek Synergy™ H1 Microplate Reader. Lysates were then resolved on 10% acrylamide gels by SDS-PAGE and transferred electrophoretically to nitrocellulose membrane (Bio-Rad) at 160 mA for 80 min. The blots were blocked in TBST buffer (10 mM Tris—HCl, pH 8, 150 mM NaCl, 0.2% Tween 20) containing 5% (w/v) nonfat dry milk for 60 min, and then incubated with the specific primary antibody diluted in blocking buffer at 4 °C overnight. Membranes were washed three times in TBST and incubated with horseradish peroxidase-conjugated secondary antibody for 1 h at room temperature. Membranes were washed 3 times and developed using enhanced chemiluminescence substrate (Pierce).

### Protein-gene expression correlation analysis

The breast cancer dataset (TCGA-BRCA), including gene expression profiles and protein expression data based on reverse phase protein arrays (RPPAs), was downloaded from UCSC Xena (<https://xenabrowser.net/datapages/>). The gene expression levels were converted from fragments per kilobase of exon model per Million mapped fragments (FPKM) to transcripts per kilobase of exon model per million mapped reads (TPM) with log<sub>2</sub>-transformation. Patient samples with both types of data ( $n = 719$ ) were included for the downstream analysis. Expression correlations were estimated using Pearson correlation coefficients. All statistical analyses were performed using R software (version 4.0.3, <https://cran.r-project.org/>), and data visualizations were attained by R package ggpubr (version 0.4.0).  $P < 0.05$  was considered statistically significant.

### Survival analyses and clinicopathologic features in clinical cohorts of breast cancer

The correlations of mRNA expression of different genes were analyzed via cBioPortal using the Provisional Metastatic Breast Cancer Project dataset (February 2020). Survival analyses were performed using the Breast Cancer Integrative Platform (<http://www.omicsnet.org/bcancer/database>). The associations of YB1 expression with patient recurrence-free survival (RFS) was assessed using the

GSE1456\_GPL96 dataset, including a total of 157 breast cancer cases with clinical follow-up. The association of Akt3 with patient RFS was assessed using the GSE2034\_GPL96 dataset, including a total of 286 breast cancer cases with clinical follow-up.

### 3D cultures

3D cultures were prepared as previously described.<sup>5</sup> Briefly, 96-well plate (Corning #3610) were coated with growth factor-reduced Matrigel (BD Biosciences) and allowed to solidify for 30 min. 1,500–3,000 cells in assay medium were seeded on Matrigel-coated 96-well plate. Assay medium contained DMEM or RPMI 1640 supplemented with 10% FBS and 2% Matrigel. The assay medium was replaced every 3–4 days.

### Mammosphere formation assay

For 1st generation of mammosphere formation, cells were seeded to ultra-low attachment 6-well plate (Corning 3471) with cell density of 2000 and 2500 cells per well for MCF10-DCIS and MDA-MB-231 cells, respectively. Cells were cultured in mammosphere medium, containing DMEM/F12 supplemented with B27 (Gibco 12587010) and 20 ng/mL EGF (R&D 236-EG), for 7–9 days. Images of mammospheres were captured by the Nikon Eclipse Tis2 microscope at 4X magnification objective. Number of mammospheres with diameter  $\geq 50 \mu\text{m}$  were counted using the Nikon NIS-Elements D software. To perform 2nd or 3rd generation mammosphere formation assay, mammospheres from 1st or 2nd generation were collected, dissociated by trypsin, and washed by mammosphere medium once. All cells were then seeded to a new ultra-low attachment 6-well plate with similar densities and cultured for 7–9 days.

### *In vitro* limiting dilution assay

Cells were seeded on wells of a 96-well, ultra-low attachment plate (Corning #3474) at the following densities: 25, 50 and 100 cells/well. Cells were cultured in mammosphere medium for 10 days. Mammospheres formed in each well were captured by the Nikon Eclipse Tis2 microscope at 4X magnification objective. Only mammospheres with diameter  $\geq 50 \mu\text{m}$  were counted using the Nikon NIS-Elements D software. CSC frequencies and *P*-value were calculated using the Online tool ELDA (<http://bioinf.wehi.edu.au/software/elda/>).

### Flow cytometry

$1 \times 10^6$  cells in PBS are incubated with CD44-PE (BD,#555479) and CD24-647 (BD,#561644) at 4 °C for 30 min in dark. Cells were washed and then analyzed by Beckman Coulter CytoFLEX S Flow cytometer analyzer. Isotype controls were used to set the threshold for positive signals.

### AldeRed ALDH detection assay

AldeRed ALDH Detection Assay kit (Merck, #SCR150) was used to detect ALDH activity of cells according to the

manufacturer's instruction. Briefly,  $2 \times 10^5$  cells were incubated with AldeRed reagent and verapamil for 35 min in 37 °C, protected from light. Cells were centrifuged and pellets were resuspended with 0.5 mL ice-cold ALDE-Red buffer on ice. ALDE-Red signal was detected by Beckman Coulter CytoFLEX S Flow cytometer analyzer, using ECM detector (610/20 BP). DEAB was used as a negative control to establish baseline fluorescence.

### RT-qPCR

Total RNA from 2D culture were extracted using RNeasy Plus Mini kit (Qiagen #74134) following the manufacturer's instruction. Reverse transcription was performed using Taq-Man Reverse Transcription Reagents (Applied Biosystems, N8080234). Quantitative RT-PCR was performed using a QuantStudio 12K Flex Real-Time PCR System (Applied Biosystems).

### *In vitro* kinase assays

Cells were transfected with vector CTL, Flag-YB1 WT, SA or SD. Twenty-four hours post-transfection, cells were serum-starved for 16 h. YB1 was immunoprecipitated from cell extracts, and then incubated with 500 ng recombinant Akt1, Akt2 or Akt3 (Sigma–Aldrich) in the presence of 250  $\mu\text{M}$  cold ATP in a kinase buffer for 1 h at 30 °C. The kinase reaction was stopped by the addition of SDS-PAGE loading buffer, and the samples were assayed by immunoblotting.

### Xenograft studies

Female nude mice (6–8 weeks old) were purchased from the laboratory animal services center, Chinese University of Hong Kong. All mice were in good health status. All procedures were approved by the Animal Ethics Committees at City University of Hong Kong, and conform to the government guidelines for the care and maintenance of laboratory animals. Randomization was used to allocate experimental units to control and treatment groups. Ear tags with unique number were used for labelling mice. For *in vivo* limiting dilution assays, cells pretreated with or without 100 ng/mL dox were seeded and cultured in 3D for 6 days. Spheroids were then collected, dissociated by trypsin and cells were resuspended in 50% Matrigel/PBS. 300, 1,200, or 4800 cells were implanted into mammary fat pad (MFP) of nude mice. Tumor formation was examined every 3–5 days. Online tool ELDA was used to calculate tumor-initiating cell frequency.

### Author contributions

Y.T. designed the experiments, performed data collection and analysis, and wrote the manuscript. J.L., T.C. and V.T. designed the experiments, and performed data collection as well as analysis. C.G.L. advised on the experimental design and data interpretation. X.W. performed data analysis and interpretation. Y.R.C. advised on the experimental design, assisted with manuscript writing and supervised the study.

## Conflict of interests

The authors have declared that no competing interest exists.

## Funding

This study was supported by General Research Fund (No. 11101517 to Y.R.C.) from the Research Grants Council (RGC) of the Hong Kong Special Administrative Region, the National Natural Science Foundation of China (No. 81972781 to Y.R.C.), Research Impact Fund (R1020-18F to Y.R.C., R4017-18 to X.W.) and Areas of Excellence Scheme (AoE/M-401/20 to X.W.) from RGC, Guangdong Basic and Applied Basic Research Foundation (No. 2019B030302012 to X.W.), Shenzhen Science and Technology Innovation Commission (No. JCYJ20200109120425045 to X.W.), and the Tung Foundation (No. 9609302 to Y.R.C.).

## Acknowledgements

The authors thank the animal facility at City University of Hong Kong for their technical support with xenograft studies; and members of the Chin laboratory for discussions.

## Appendix A. Supplementary data

Supplementary data to this article can be found online at <https://doi.org/10.1016/j.gendis.2022.08.006>.

## References

1. Lee KL, Kuo YC, Ho YS, Huang YH. Triple-negative breast cancer: current understanding and future therapeutic breakthrough targeting cancer stemness. *Cancers (Basel)*. 2019;11(9):1334.
2. Chin YR, Yoshida T, Marusyk A, Beck AH, Polyak K, Toker A. Targeting Akt3 signaling in triple-negative breast cancer. *Cancer Res*. 2014;74(3):964–973.
3. Sutherland BW, Kucab J, Wu J, et al. Akt phosphorylates the Y-box binding protein 1 at Ser102 located in the cold shock domain

and affects the anchorage-independent growth of breast cancer cells. *Oncogene*. 2005;24(26):4281–4292.

4. Evdokimova V, Ruzanov P, Anglesio MS, et al. Akt-mediated YB-1 phosphorylation activates translation of silent mRNA species. *Mol Cell Biol*. 2006;26(1):277–292.
5. Debnath J, Muthuswamy SK, Brugge JS. Morphogenesis and oncogenesis of MCF-10A mammary epithelial acini grown in three-dimensional basement membrane cultures. *Methods*. 2003;30(3):256–268.

Ye Tian

Jiang Li

Tsz Chung Cheung

Vincent Tam

*Tung Biomedical Sciences Centre, Department of Biomedical Sciences, City University of Hong Kong, Kowloon, Hong Kong SAR, China*

C. Geoffrey Lau

*Department of Neuroscience, City University of Hong Kong, Kowloon, Hong Kong SAR, China*

Xin Wang

*City University of Hong Kong Shenzhen Research Institute, Shenzhen, Guangdong 518057, China*

*Department of Surgery, The Chinese University of Hong Kong, Shatin, Hong Kong SAR, China*

Y. Rebecca Chin\*

*Tung Biomedical Sciences Centre, Department of Biomedical Sciences, City University of Hong Kong, Kowloon, Hong Kong SAR, China*

*City University of Hong Kong Shenzhen Research Institute, Shenzhen, Guangdong 518057, China*

\*Corresponding author. Tung Biomedical Sciences Centre, Department of Biomedical Sciences, City University of Hong Kong, Kowloon, Hong Kong SAR, China.

*E-mail address: rebecca.chin@cityu.edu.hk (Y.R. Chin)*

18 May 2022

Available online 1 September 2022